Comparison of K-doped and pure cold-rolled tungsten sheets: Microstructure restoration in different temperature regimes

Philipp Lied[1], Wolfgang Pantleon[2], Carsten Bonnekoh[1], Michael Dürrschnabel[1], Christian Bienert[3], Andreas Hoffmann[3], Jens Reiser[1], Michael Rieth[1]

1) Karlsruhe Institute of Technology, Institute for Applied Materials – Applied Materials Physics, 76344 Eggenstein-Leopoldshafen, Germany

2) Technical University of Denmark, Department of Civil and Mechanical Engineering, Section of Materials and Surface Engineering, 2800 Kongens Lyngby, Denmark

3) Plansee SE, 6600 Reutte, Austria

Abstract

For tungsten in divertor parts of future fusion reactors, a fine-grained microstructure is preferred to reduce its brittle-to-ductile transition temperature and minimize cracking events due to cyclic thermal and mechanical loading. In our ongoing study on tungsten sheets with different degree of deformation by warm- and cold-rolling, the potential of potassium-doping to stabilize the microstructure at high operation temperatures is assessed. Successful production of technically pure and equivalently rolled potassium-doped tungsten sheets up to very high logarithmic strains of 4.6 was already shown in the past with in-depth analysis of the evolution of microstructure and mechanical properties after rolling steps. Our current study investigates the microstructure changes in the same material batch by recovery, recrystallization and grain growth in temperature regimes between 600 °C and 2400 °C. Annealing studies with subsequent microhardness and SEM analysis reveal increased retardation of recrystallization in potassium-doped tungsten with higher rolling strain, but abnormal grain growth at high temperatures is also increased. However, potassium-doped tungsten with low rolling strain shows promising results with much less grain growth than its pure tungsten counterpart.

Graphical Abstract

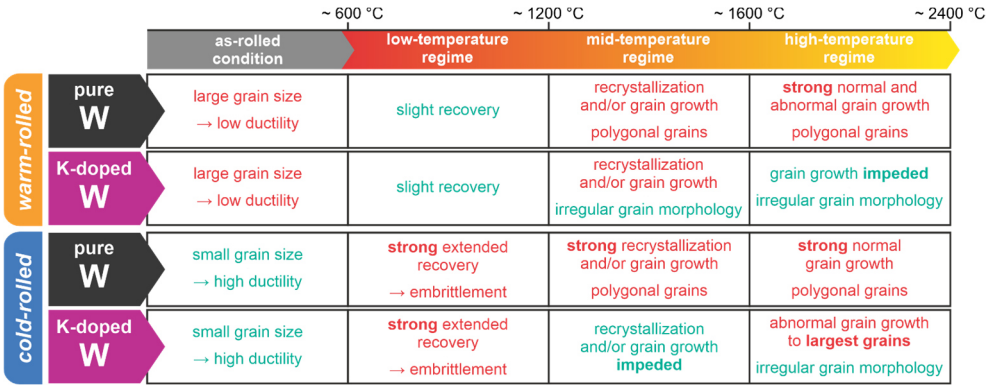

Highlights

- Cold-rolled tungsten sheets heavily prone for extended recovery at low temperatures
- K-doping impedes recrystallization and grain growth of W in mid-temperature regime
- Increasing rolling strain improves K-bubble dispersion and inhibition of RX/GG
- However, high K-bubble dispersion leads to abnormal GG at high temperatures
- K-doped W with low rolling strain shows smallest grain size at high temperatures

Keywords

fusion reactor materials, extended recovery, recrystallization, grain growth, electron backscatter diffraction, hardness indentation

1 Introduction

Tungsten is the most promising material for the use in parts of future fusion power reactors, where highest heat and neutron irradiation loads occur. It possesses the highest melting point among all elements with 3420 °C [1], low vapour pressure in the plasma and high wear resistance. This is accompanied by good high-temperature strength and – of major importance for heat exchange components as the divertor – good thermal conductivity. One of the major drawbacks, however, is its high ductile-to-brittle transition temperature (DBTT) in the range of 600 °C [2], which can result in premature failure of components under cyclic heat loads during the lifetime of the reactor [3]. In the past, multiple studies demonstrated that cold-rolling of tungsten can lead to a drastically reduced DBTT [4–7], even below room temperature [8]. This reduction is considered to be caused by a significant increase of grain boundary density in the tungsten microstructure. However, it was also shown that for a sufficient description of the dependence of the DBTT by a Hall-Petch relation, not only high-angle but also low-angle boundaries have to be taken into account [9].

While the mechanical properties can be improved by the reduction of the grain size, the thereby created microstructure is unstable at high temperatures due to recovery, recrystallization and grain growth [10–13]. By that, the initially decreased DBTT after cold-working is increased again and embrittlement is observed [14]. For tungsten, multiple approaches have been investigated to impede of grain coarsening at high temperatures. These include e.g. forming solid solutions of tungsten with other refractory metals [15–17], incorporation of oxides [18, 19] and carbides [20–22], as well as doping with potassium (K) [16, 17, 23–25]. K-doping of W is an established process in the industry for incandescent lamp wires since many decades. It leads to formation of finely dispersed pores, tens of nanometres in size, which are filled with potassium (“K-bubbles”) and act as strong barriers against glide of dislocations and grain boundary migration [23]. The latter approach is used in this study, primarily to combine the high ductility of cold-rolled W sheets with a stabilized microstructure.

The leading questions for our ongoing study are: Which microstructure restoration phenomena occur in tungsten with low and high rolling strain? And how are these phenomena influenced by K-doping? Previously published annealing experiments between 700 °C and 2200 °C (1 h) with subsequent analysis by microhardness testing already indicated certain temperature regimes in which recovery, recrystallization or grain growth dominate [10]. In the mid-temperature regime around 1200 °C to 1600 °C recrystallization occurs and K-doping shows a strong retarding effect in W sheets with high degree of deformation due to increased distribution of K-bubbles by rolling. In a lower temperature regime, the cold-rolled W sheets show extended recovery [10], which is the main cause of embrittlement at low temperatures [14]. Since a significant loss of hardness was already observed after annealing at the lowest investigated temperature, the question whether extended recovery occurs even below 700 °C is still open. In addition, the matter of grain growth at high temperatures has not yet been addressed in detail, which is important in the light of high thermal load events by plasma instabilities in the reactor, such as edge-localized-modes (ELMs) or disruptions [26]. Therefore, additional data are presented herein to contribute to the preceding study [10] to allow for a more detailed evaluation of the recovery phenomena in the low temperature regime as well as the grain growth phenomena in a high temperature regime.

2 Materials and methods

For this study, we used the same set of materials as in former studies [10, 27]. These material sets have been produced from two sintered ingots at PLANSEE SE (Reutte, Austria): (i) K-doped tungsten, (commercially available as “WVM”) with a K-content of 60 ppm and (ii) technically pure tungsten (> 99.97 wt.% W). Although pure tungsten and K-doped tungsten are commercially available, the rolling to very high degrees of deformation is a rather new approach [28] and has been further advanced in our preceding study [10] to sheets of 50 µm thickness (thickness

reduction of more than 99 %, equals logarithmic strain of 4.6). After shaping the sintered ingot by hot-rolling, the sheets WK1.6 (with 1.03 mm thickness), WK2.7 (0.35 mm) and WK3.1 (0.22 mm) were produced by warm-rolling and separation. After that, the production continued with cold-rolling to form the sheets WK3.7 (0.127 mm) and WK4.6 (0.052 mm). The same procedure was applied to the pure W ingot to create the sheets WP1.6 (1.09 mm), WP2.7 (0.36 mm) and WP3.3 (0.19 mm) by warm-rolling as well as WP3.7 (0.134 mm) and WP4.7 (0.051 mm) by cold-rolling. More details about the production, chemical composition, grain size distribution and texture as well as tensile tests and fracture toughness tests in the as-rolled condition can be found in the preceding studies [10, 27].

Isochronal temperature treatments between 500 °C up to 1270 °C for 1 h were done at KIT with a Nabertherm LHT 08/18 furnace (where specimens were encapsulated in evacuated quartz glass ampoules to prevent oxidation), while annealing from 1400 °C up to 2400 °C for 1 h was performed at PLANSEE SE in hydrogen atmosphere (as well as the isothermal annealing series at 2200 °C). Ampoules with pure and K-doped W were annealed simultaneously in the same furnace to guarantee the same temperature treatment. For annealing in hydrogen atmosphere, the samples of pure and K-doped W were treated separately in order to avoid cross-contamination of doped elements. Additional isothermal annealings of specimens in glass ampoules were conducted at 750 °C for various times between 1 h and 1000 h.

For Vickers hardness testing, a Clemex CMT.HD indenter has been used with a test load of 0.981 N (100 g, HV0.1). The hardness indentation was performed on the polished faces of embedded sheets on the RD × ND plane (i.e. along transversal direction). At least seven points have been measured in different areas of every sample for calculation of arithmetic mean and standard deviation of the distribution.

Microstructure analysis by scanning electron microscopy (SEM) in addition to electron backscatter diffraction (EBSD) has been performed on polished cross sections containing the rolling direction (RD) and normal direction (ND) of the W sheets. This surface has been prepared by grinding, polishing and subsequent electropolishing with aqueous NaOH solution. For SEM analysis a Zeiss Merlin field-emission-gun scanning electron microscope equipped with an EDAX Hikari high-speed EBSD camera was used. For an overview of the microstructure, a detector for backscattered electrons was chosen to distinguish grains by orientation contrast. The SEM acceleration voltage was set to 20 kV with a probe current of 10 nA. EBSD data were acquired as hexagonal pixel grids. Data evaluation was performed with EDAX OIM Analysis v7.3.1. For grain size calculations, boundaries with disorientation angles above 15° between neighbouring pixels are defined as high angle boundaries (HABs), while boundaries with disorientation angles between 2°-15° are considered as low angle boundaries (LABs). Orientation distribution functions (ODF) are calculated using harmonic series expansion up to rank 34.

3 Results and discussion

3.1 Isochronal annealing for 1 h between 500 °C and 2400 °C

Annealing experiments in a previous study [10] already indicated a severe loss of hardness after 1 h at 700 °C for W sheets with high degree of deformation. For a more detailed examination, we extended the dataset for these isochronal annealing series by the annealing temperatures 500 °C, 600 °C and 750 °C for 1 h. The combined results from hardness measurements are presented in Figure 1. As seen already in the preceding study, the curves of the Vickers hardness after annealing at different temperatures show two distinct drops. By that, three different temperature regimes can be distinguished from the hardness loss curve (Figure 1). These regimes should not be understood as strictly separated by sharp boundaries and are only used herein to simplify the following discussion, since the onset for specific restoration phenomena is difficult to define and the temperature regimes at which they occur overlap. Also, it should be emphasised that the isochronal annealing experiments here are limited to 1 h and that microstructure restoration can occur at lower temperatures with longer annealing times. This should be considered when the lifetime of divertor components during two years of full power operation is discussed [29].

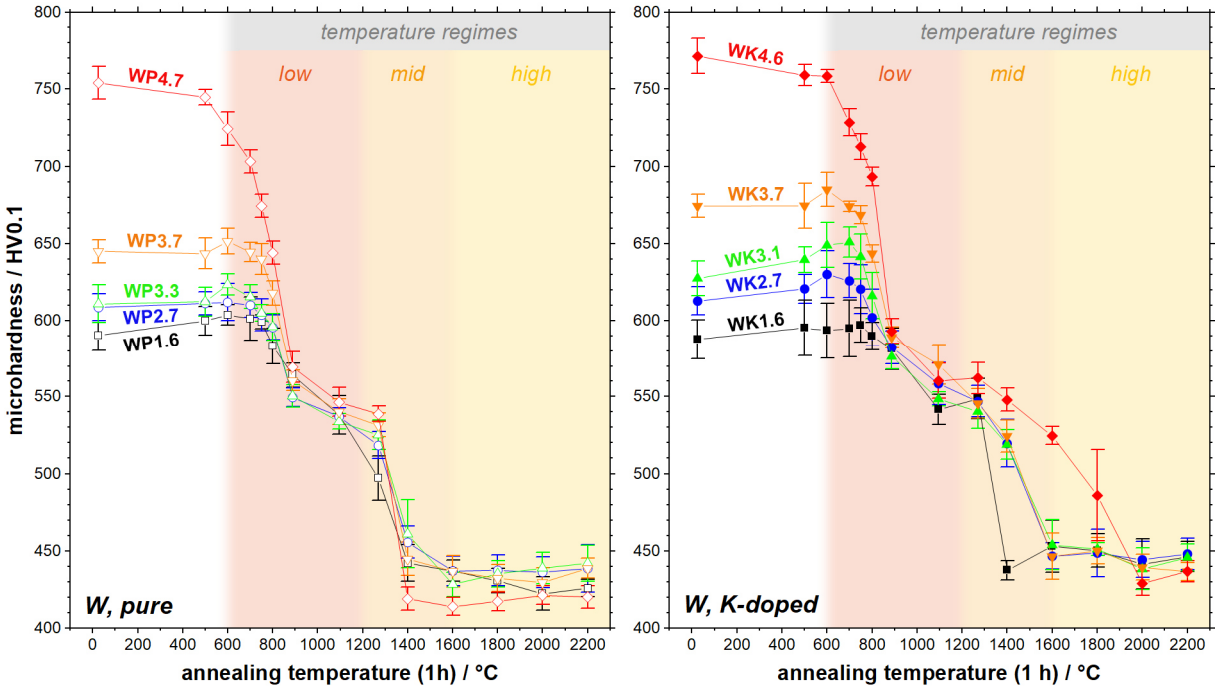

Figure 1: Microhardness values of pure W and K-doped W with different rolling strain after annealing for 1 h in dependence on annealing temperature. Three temperature regimes are distinguished, as discussed in the text. Error bars represent the range of the standard deviation of at least seven indentations per sample.

In the regime at low temperatures (Figure 1, highlighted in red), most samples with a lower degree of deformation show a slight increase of hardness compared to the as-rolled condition and specimens annealed at 500 °C. This “bump” in the hardness curve could indicate an onset of recovery, where mobile dislocations are annihilated first, leading to slight hardening. After annealing at 800 °C a drop is observed in general. However, for the sheets with highest degree of deformation, this drop is already observed at 700 °C for WK4.6 and 600 °C for WP4.7 without an initial increase of hardness. An explanation could be the very high dislocation density in these sheets (see TEM results in [10]), causing a high driving force for recovery and a rapid decrease of both mobile and less mobile dislocations such that a potential increase in flow stress due to the lack of mobile dislocations is compensated by the loss in strength due to annihilation of less mobile ones.

Interestingly, the new data show that recovery mechanisms are already triggered at a temperature of about 600 °C. The decrease of hardness is most severe after annealing at 900 °C, especially for the sheets with highest rolling strain. At this temperature, the hardness for all five pure W sheets can be found on a similar level around 560±10 HV0.1 and for the K-doped W sheets around 585±10 HV0.1. As stated before [10], the reason for the drastically reduced hardness of the sheets with highest rolling strain in the low temperature regime is attributed to extended recovery. During such extended recovery, gradual coarsening of grains is observed as seen for the microstructure of both thinnest sheets WP4.7 and WK4.6 after isothermal annealing at 750 °C between 1 h to 1000 h (Figure 2). The same characteristic feature of extended recovery is also revealed by EBSD on samples e.g. annealed at 1270 °C for 1 h (Figure 3). The latter annealing condition represents an interesting transition between the low- and mid-temperature regime, where recovery is almost completed (see stagnant decrease in hardness from 900 °C to 1270 °C for most samples in Figure 1), while nuclei from recrystallization presumably just started to grow (see second drop in hardness for most samples at next higher temperature of 1400 °C in Figure 1). For the same annealing condition of 1 h at 1270 °C, the microstructure of the K-doped sheet with lowest degree of deformation (WK1.6) in Figure 3b clearly shows starting of recrystallization by formation of nuclei with random orientation (cf. ODF section in Figure 3b). In contrast, the thinnest sheet WK4.6 affected by extended recovery shows (i) significant coarsening of the microstructure, which occurs evenly across the sample volume, (ii) a retainment of the strong rolling texture (compare to texture shown in [10]) and (iii) no observable signs of recrystallization by formation of nuclei up to this

temperature (Figure 3a). This phenomenon is sometimes described in literature as “recrystallization in-situ” or “continuous recrystallization” and is often observed in materials with high degree of deformation [30]. As in the former study [10], new data confirmed as well that extended recovery occurs in similarly cold-rolled W sheets with high degree of deformation and 80 ppm K [12].

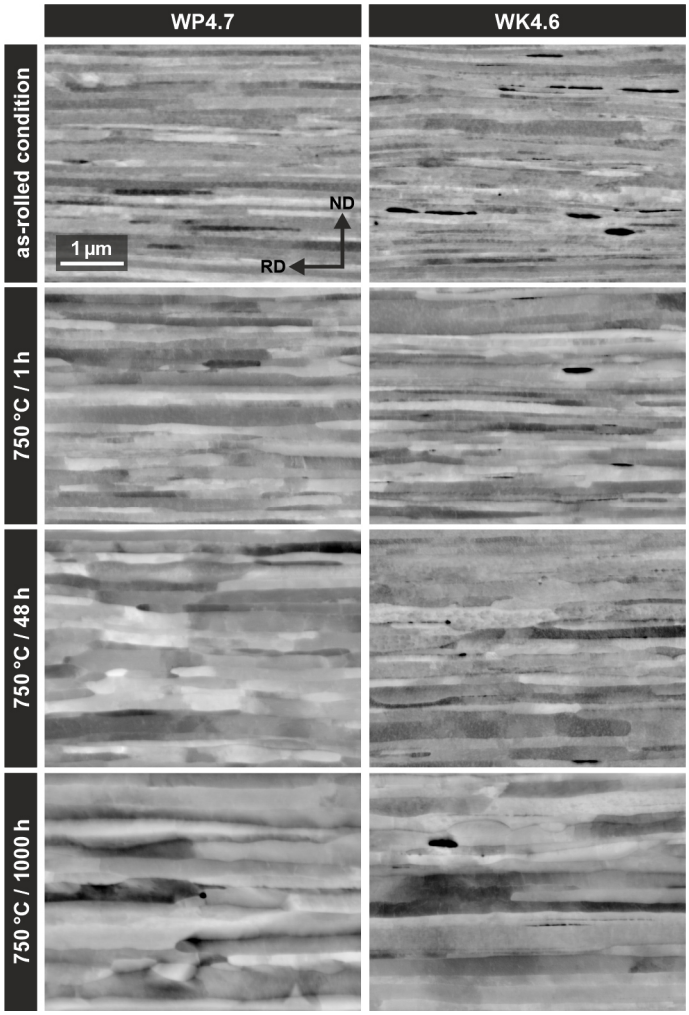

Figure 2: Microstructure of the two tungsten sheet with highest degree of deformation WP4.7 and WK4.6 in as-rolled condition and after isothermal annealing at 750 °C for 1 h, 48 h and 1000 h.

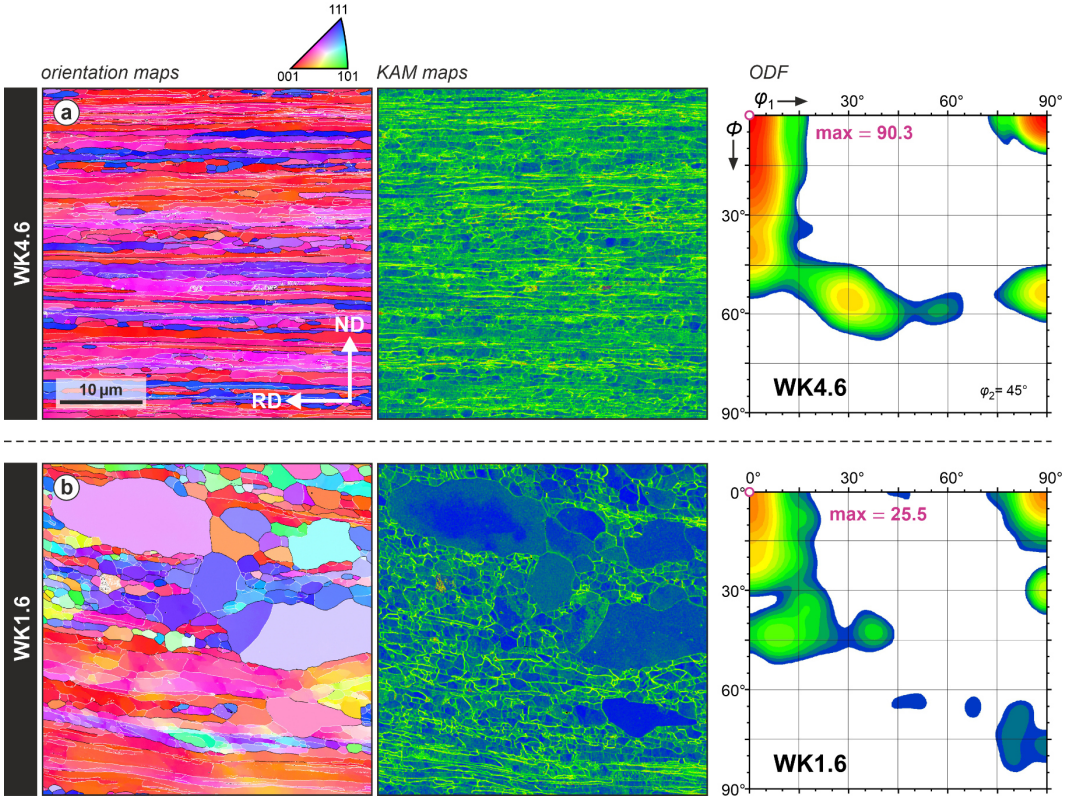

Figure 3: Orientation maps and kernel average misorientation (KAM) maps from EBSD measurements for the K-doped sheets WK4.6 (a) and WK1.6 (b), both after annealing at 1270 °C for 1 h in sections containing normal direction (ND) and rolling direction (RD). Regions of high local disorientations appear green in the KAM maps, whereas newly recrystallized grains appear blue. The respective orientation distribution functions (ODF) are on the right-hand side with maximum values given as multiples of a random distribution.

In the mid-temperature regime (Figure 1, highlighted in orange), a second decrease of hardness is observed, which is most severe after annealing at 1400 °C for all samples of pure W. At this temperature, the hardness is settled around 410 to 460 HV0.1, approaching the hardness of W single crystals [2]. As already indicated by EBSD for the sheets with low degree of deformation in Figure 3, the hardness loss in this temperature regime above 1200 °C is mainly caused by recrystallization. However, for the sheets with high degree of deformation, where extended recovery presumably occurred in the early stages of annealing, it is unclear if nuclei for primary recrystallization can even develop or if grain growth is the dominating restoration phenomenon. Yet, SEM analysis in the preceding study [10] shows a coarse microstructure in pure W after annealing at 1400 °C with a grain size of several tens of micrometres and grains of polygonal shape. On the other hand, K-doped W with high degree of deformation reveals a much finer microstructure (Figure 16 in [10]), which is similar to the microstructure observed after annealing at 1270 °C for WK4.6 (Figure 3). The different microstructure is also reflected in the hardness curves (Figure 1), where the samples of K-doped W show a different behaviour at 1400 °C than the samples of pure W: Except for WK1.6, which is found to have a hardness in the same range than the pure W sheets at this temperature, all sheets with higher degree of deformation have maintained a higher hardness with about 520 HV0.1 for WK2.7, WK3.1 and WK3.7 or even about 550 HV0.1 for WK4.6. The latter also maintains a higher hardness at 1600 °C (and even at 1800 °C), for which the hardness of all other sheets decreased to about 450 HV0.1. This indicates that a retardation of recrystallization and/or grain growth by K-doping occurs, which becomes increasingly effective with higher degree of deformation and can be attributed to an improved distribution of K-bubbles with increasing rolling strain [10].

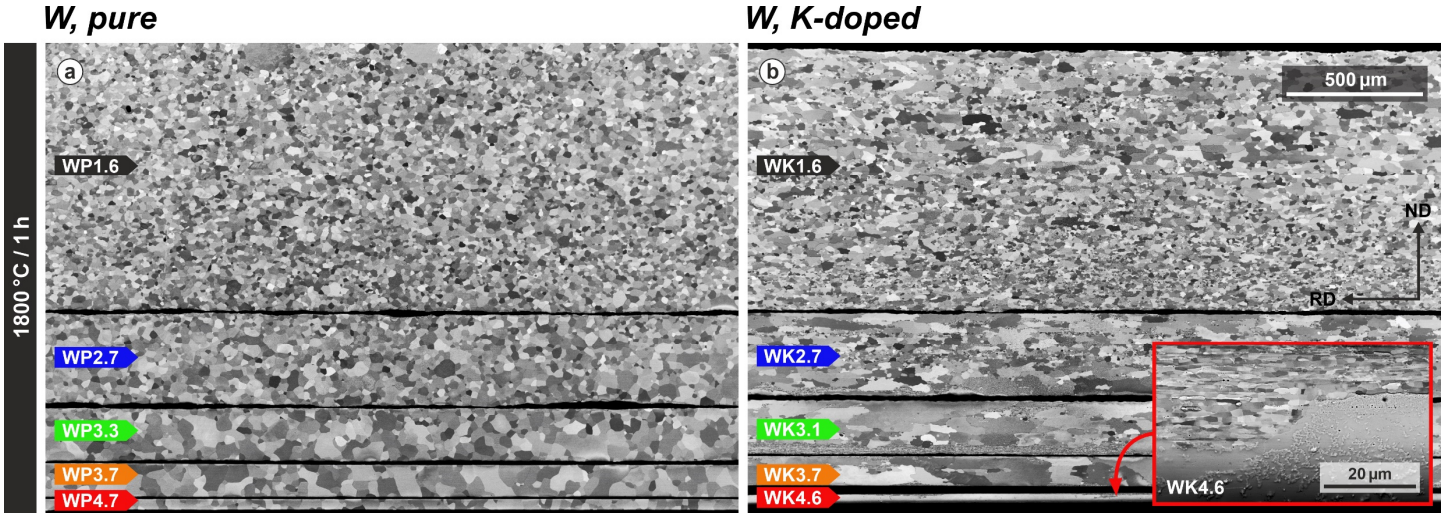

Figure 4: Microstructure of (a) the pure W sheets WP1.6, WP2.7, WP3.3, WP3.7, WP4.7 (from top to bottom) and (b) the K-doped sheets WK1.6, WK2.7, WK3.1, WK3.7, WK4.6 after annealing at 1800 °C for 1 h. The red inset shows enlargement of the 50 µm thick sheet WK4.6.

The high standard deviation for the data point of WK4.6 at 1800 °C indicates heterogeneities as they may occur in case of a bimodal grain size distribution. A reason for that can be abnormal grain growth in the high-temperature regime, which is a peculiar phenomenon observed in K-doped incandescent lamp wires [31]. SEM imaging of the samples annealed at 1800 °C confirms that abnormal grain growth indeed leads to much coarser grains for the K-doped sheets with high deformation (Figure 4). The K-doped sheet with lowest rolling strain seems to be unaffected by this phenomenon as well as the complete set of pure W sheets, for which the grain size has a unimodal distribution. Unfortunately, different extend of grain growth in this temperature regime cannot be resolved by the hardness measurements with HV0.1, as the grain size is often found to be larger than 100 µm for all samples, whereas the size of indents by the measurement is in the range of only up to 25 µm. This circumstance results in similar hardness values close to the hardness of a W single crystal for all sheets in this temperature regime, despite that the microstructure can differ significantly. Therefore, SEM analysis is used in the following for several samples of an isothermal annealing study at 2200 °C to investigate the evolution of grain size and morphology.

3.2 Annealing at 2200 °C

For the following investigation, samples were heat treated for 2 h or 8 h at 2200 °C. The SEM images of all investigated samples (Figure 5) show a high variation in the progression of grain growth for pure and K-doped W, which are discussed in the following.

After annealing for 2 h at 2200 °C, pure W reveals grains of polygonal shape (Figure 5a). The sheets with low rolling strain show a drastically coarsened microstructure by grain growth compared to after annealing for 1 h at 1800 °C (Figure 4a), where complete recrystallization was observed. On the contrary, the thinnest sheets show only slight coarsening, which could be due to increased grain boundary pinning at the surfaces of the sheets with decreasing sample thickness. Additionally, the thickest pure W sheet WP1.6 exposes several grains surpassing the size of their neighbouring grains by multiple times. With longer annealing time, such grains grow to sizes above 1 mm along rolling direction (Figure 5c). Abnormally large grown grains are also found in WK2.7 (not in the area shown here). These observations demonstrate that abnormal grain growth does not only occur in the highly deformed K-doped sheets, but also in late stages of annealing in pure tungsten with low degree of deformation.

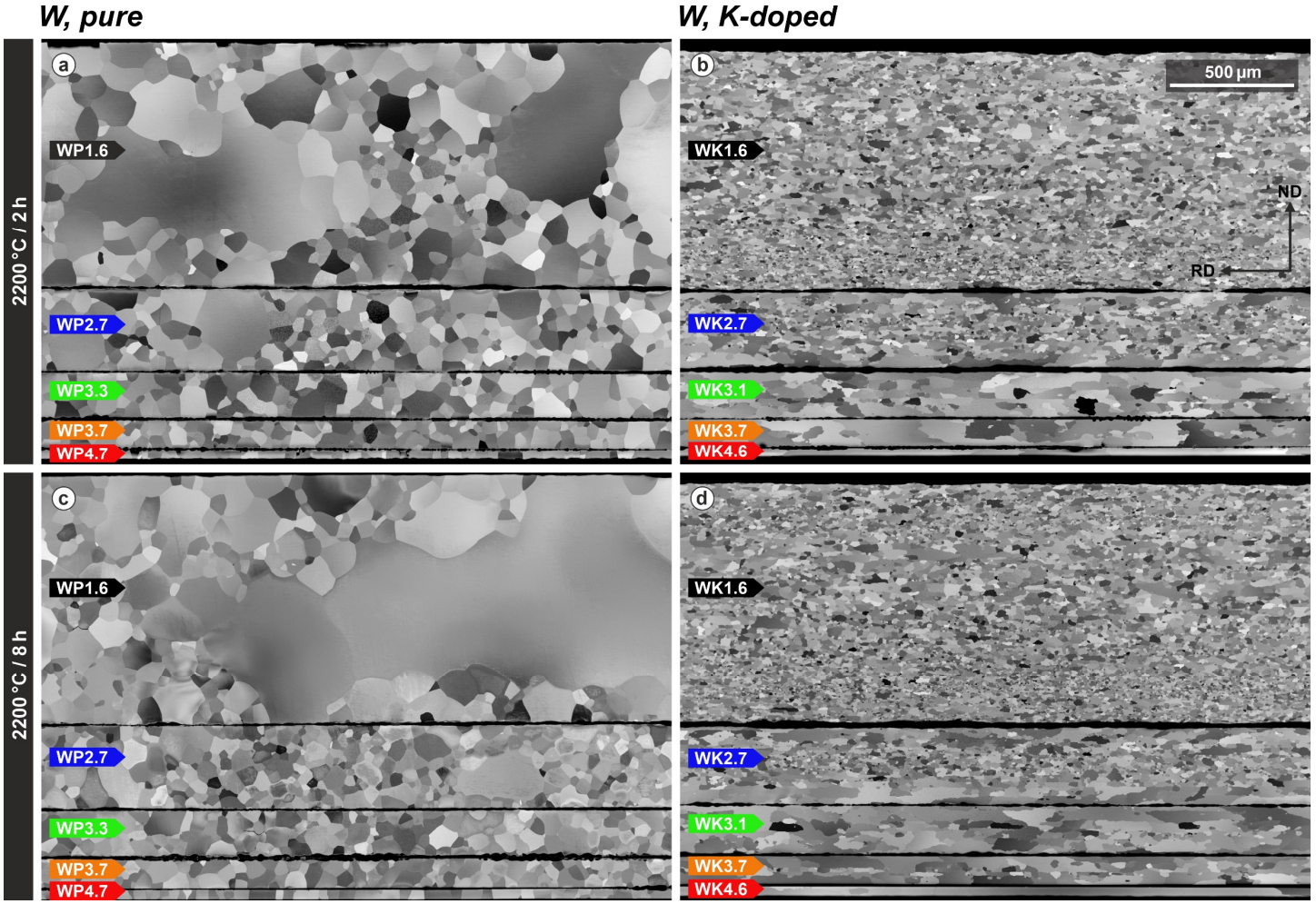

Figure 5: Microstructure of (a,c) the pure W sheets WP1.6, WP2.7, WP3.3, WP3.7, WP4.7 (from top to bottom) and (b,d) the K-doped sheets WK1.6, WK2.7, WK3.1, WK3.7, WK4.6 after annealing at 2200 °C for (a,b) 2 h and (c,d) 8 h.

In contrary to the results for pure W, the largest grain size of all the K-doped W sheets after annealing at 2200 °C is not found in the thickest, but in the thinnest sheet. In WK4.6, abnormal grain growth progressed to an extend that regions with very small grain size (as found coexisting to abnormally large grains after annealing at 1800 °C for 1 h, Figure 4b) are completely consumed. For the most part, this sheet consists of single grains across the whole thickness of the sheet, which stretch often more than 1 mm along rolling direction. On the other hand, the maximum grain size of WK1.6 (Figure 5b, d) after annealing at 2200 °C does not differ much from after annealing at 1800 °C. In fact, WK1.6 clearly has the smallest grains of all investigated specimens after annealing at 2200 °C and no significant changes can be observed between an annealing time of 2 h and 8 h.

The difference in grain size between WP1.6 and WK1.6 can be seen in the orientation maps of Figure 6. While the local texture is dominated by components of the rotated cube orientation ({001}⟨110⟩) in WP1.6, WK1.6 still shows components of the γ-fibre from the rolling texture. For an evaluation of the grain size in WP1.6, the used map size of 600 × 800 µm² is by far too small and includes not enough grains (Figure 6a). Therefore, two large orientation maps with a size of 3000 × 950 µm² (RD × ND) with a step size of 1.6 µm were obtained for WP1.6 annealed for 2 h as well as 8 h. From these two maps for each condition, grain size distribution and arithmetic mean of the grain size (Figure 7) were calculated. For the more fine-grained samples of WK1.6, the same calculations were applied to maps of 600 × 800 µm² obtained with a step size of 0.4 µm.

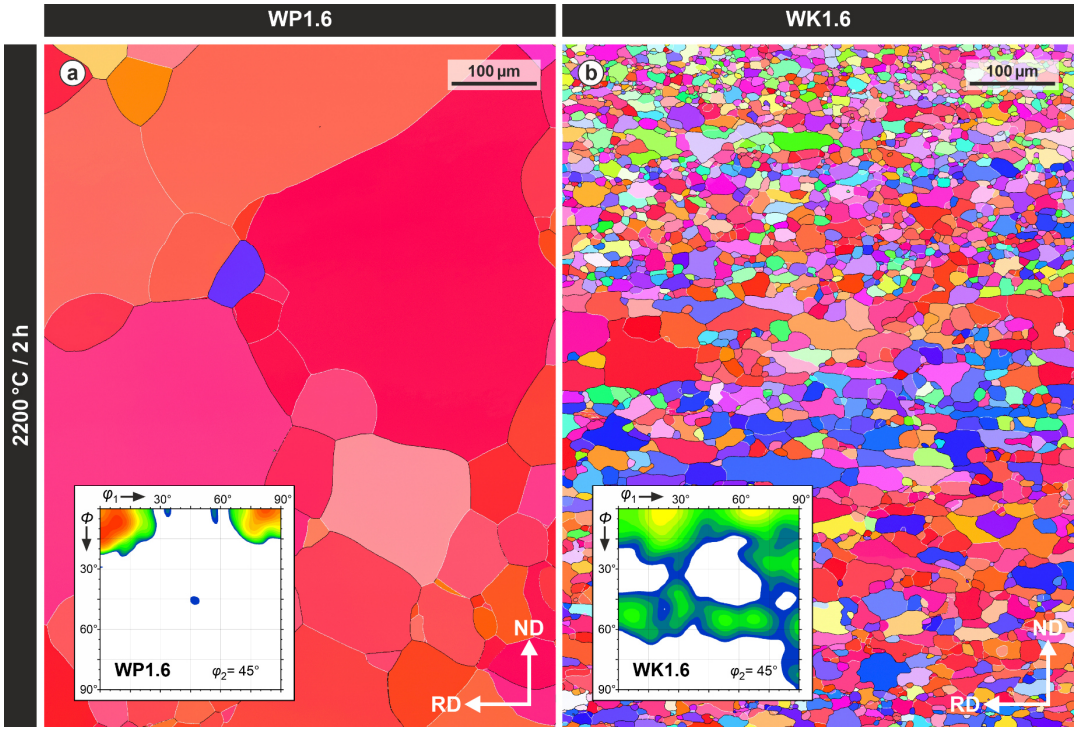

Figure 6: Orientation maps of (a) WP1.6 and (b) WK1.6 after annealing at 2200 °C for 2 h (maps size 600 × 800 µm²). HABs are drawn as black line, LABs as white line. The respective orientation distribution functions (ODF) are shown as inset.

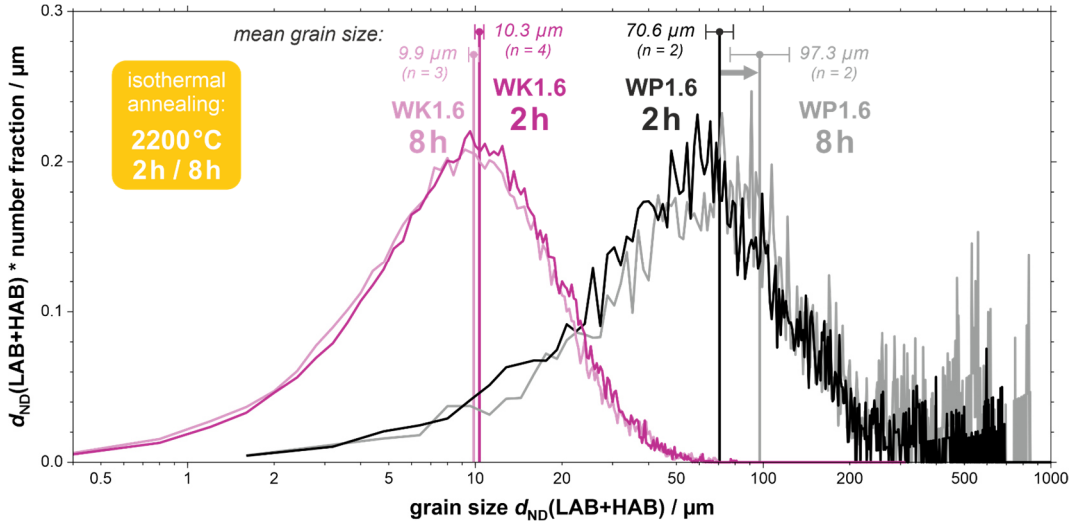

Figure 7: Distribution of the grain size along normal direction (d_{ND}) with inclusion of HAB and LAB for WK1.6 and WP1.6 after annealing at 2200 °C for 2 h and 8 h, respectively (i.e. all boundaries > 2° are considered). The number fraction is multiplied with d_{ND} in order to highlight large grains, which are low in number but cover a large area, and to better indicate a bimodal size distribution. Note that the number fraction of WP was divided by 4 to correct for a four times larger bin size used for WP1.6 due to the four times larger step size during EBSD measurement. Arithmetic means of grain sizes for WK1.6 and WP1.6 are depicted by vertical lines. The error bars indicate the standard deviation between multiple arithmetic means for n EBSD measurements for each sample condition.

The arithmetic mean of the grain size of WP1.6 (Figure 7) is seven times larger after annealing for 2 h and ten times larger after annealing for 8 h compared to the mean of the grain size of WK1.6, which does not significantly change from 2 h to 8 h (even a slight decrease is observed, which is not significant, however). It has to be noted that error bars are calculated from multiple arithmetic means for three or four orientation maps per sample. In case of WP1.6,

there are only two maps, therefore only two means, rendering the statistics insufficient. Nevertheless, the large error bars for the samples of WP1.6 indicate a high variation of observed grain sizes between different investigated sample sections and that the investigated sample sections did not contain enough abnormally grown grains to evaluate their size with sufficient statistics. Given the sheer size of such grains, this task is impractical to achieve by EBSD (Figure 5c shows the minimum magnification of the used SEM). However, in the grain size distribution of WP1.6 (Figure 7), the fraction of abnormally large grains (> 200 µm) can be viewed separately from the smaller grains (< 200 µm). Between the sample annealed for 2 h and 8 h, an increase in grains size can be seen both for abnormally large grains and for smaller grains, which indicates that besides abnormal grain growth also normal grain growth still progresses in WP1.6. Such an increase is not observed for WK1.6, giving the impression that abnormal *and* normal grain growth is strongly impeded. The reason for such a strong retardation could be attributed to K-bubble instabilities, which lead to growth of the bubbles in the high temperature regime (by accumulation of voids, driven by increased vapour pressure of K inside the bubble volume [32]) and thereby increased Zener-pinning.

4 Conclusion

The microstructure restoration phenomena observed in the investigated tungsten sheets after isochronal annealing for 1 h and isothermal annealing at 2200 °C are summarized in the graphical abstract. Although W sheets with high degree of deformation by cold-rolling have superior mechanical behaviour like ductility at room temperature, it is shown that the observed extended recovery leads to significant hardness loss, expected to cause embrittlement already in a low temperature regime. K-doping seems unable to suppress extended recovery, instead, a strong retardation of primary recrystallization and/or grain growth in the mid-temperature regime is observed in the sheets with high rolling strain. In the high-temperature regime, normal grain growth is accompanied by strong abnormal grain growth. Although such high temperatures may not be the targeted operation temperatures in a fusion reactor, they are still important when seen in the light of unwanted thermal events, which can severely damage the divertor unit. In summary, most benefits of K-doping for the microstructural evolution can be seen in the restoration behaviour of the K-doped W sheet with lowest thickness reduction. Normal and abnormal grain growth seems to be suppressed very effectively at high temperatures and the irregular grain morphology could prove advantageous against crack propagation compared to the straight polygonal boundaries of pure W.

Acknowledgements

This work has been carried out within the framework of the EUROfusion Consortium, funded by the European Union via the Euratom Research and Training Programme (Grant Agreement No 101052200 — EUROfusion). Views and opinions expressed are however those of the author(s) only and do not necessarily reflect those of the European Union or the European Commission. Neither the European Union nor the European Commission can be held responsible for them. The support of the tungsten supplier, PLANSEE SE (Reutte/Austria), is gratefully acknowledged.

References

[1] Martienssen W, Warlimont H. Springer handbook of condensed matter and materials data. Heidelberg: Springer; 2005.

[2] Lassner E, Schubert W-D. Tungsten - Properties, Chemistry, Technology of the Element, Alloys, and Chemical Compounds. New York: Kluwer Academic; 1999.

[3] Hirai T, Panayotis S, Barabash V, Amzallag C, Escourbiac F, Durocher A et al. Use of tungsten material for the ITER divertor. Nuclear Materials and Energy 2016;9:616–22.

[4] Wei Q, Kecskes LJ. Effect of low-temperature rolling on the tensile behavior of commercially pure tungsten. Materials Science and Engineering: A 2008;491(1-2):62–9.

[5] Reiser J, Hoffmann J, Jäntsch U, Klimenkov M, Bonk S, Bonnekoh C et al. Ductilisation of tungsten (W): On the increase of strength AND room-temperature tensile ductility through cold-rolling. International Journal of Refractory Metals and Hard Materials 2017;64:261–78.
[6] Bonk S, Reiser J, Hoffmann J, Hoffmann A. Cold rolled tungsten (W) plates and foils: Evolution of the microstructure. International Journal of Refractory Metals and Hard Materials 2016;60:92–8.
[7] Nikolic V, Wurster S, Firneis D, Pippan R. Improved fracture behavior and microstructural characterization of thin tungsten foils. Nuclear Materials and Energy 2016;9:181–8.
[8] Bonnekoh C, Hoffmann A, Reiser J. The brittle-to-ductile transition in cold rolled tungsten: On the decrease of the brittle-to-ductile transition by 600 K to −65 °C. International Journal of Refractory Metals and Hard Materials 2018;71:181–9.
[9] Bonnekoh C, Lied P, Zaefferer S, Jäntsch U, Hoffmann A, Reiser J et al. The brittle-to-ductile transition in cold-rolled tungsten sheets: Contributions of grain and subgrain boundaries to the enhanced ductility after pre-deformation. Nuclear Materials and Energy 2020;25:100769.
[10] Lied P, Bonnekoh C, Pantleon W, Stricker M, Hoffmann A, Reiser J. Comparison of K-doped and pure cold-rolled tungsten sheets: As-rolled condition and recrystallization behaviour after isochronal annealing at different temperatures. International Journal of Refractory Metals and Hard Materials 2019:105047.
[11] Reiser J, Bonnekoh C, Karcher T, Pfleging W, Weygand D, Hoffmann A. Recrystallisation towards a single texture component in heavily cold rolled tungsten (W) sheets and its impact on micromechanics. International Journal of Refractory Metals and Hard Materials 2020;86:105084.
[12] Tarras Madsen D, Ciucani UM, Hoffmann A, Pantleon W. Thermal stability of thin rolled potassium-doped tungsten sheets during annealing at temperatures up to 1400 °C. Nuclear Materials and Energy 2022:101126.
[13] Tarras Madsen D, Ciucani UM, Hoffmann A, Pantleon W. Strong rotated cube textures in thin cold-rolled potassium-doped tungsten sheets during annealing up to 1300 °C. IOP Conf. Ser.: Mater. Sci. Eng. 2021;1121(1):12018.
[14] Bonnekoh C, Lied P, Pantleon W, Karcher T, Leiste H, Hoffmann A et al. The brittle-to-ductile transition in cold-rolled tungsten sheets: On the loss of room-temperature ductility after annealing and the phenomenon of 45° embrittlement. International Journal of Refractory Metals and Hard Materials 2020;93:105347.
[15] Rieth M, Reiser J, Dafferner B, Baumgärtner S. The Impact of Refractory Material Properties on the Helium Cooled Divertor Design. Fusion Science and Technology 2012;61(1T):381–4.
[16] Hasegawa A, Fukuda M, Tanno T, Nogami S, Yabuuchi K, Tanaka T et al. Neutron irradiation effects on grain-refined W and W-alloys. Toki, Gifu, Japan; 2014.
[17] Nogami S, Hasegawa A, Fukuda M, Watanabe S, Reiser J, Rieth M. Tungsten modified by potassium doping and rhenium addition for fusion reactor applications. Fusion Engineering and Design 2020;152:111445.
[18] Wesemann I, Spielmann W, Heel P, Hoffmann A. Fracture strength and microstructure of ODS tungsten alloys. International Journal of Refractory Metals and Hard Materials 2010;28(6):687–91.
[19] Leichtfried G. Molybdenum lanthanum oxide: Special material properties by dispersoid refining during deformation. Advances in Powder Metallurgy 1992;9(January 1992):123–38.
[20] Jenuš P, Iveković A, Kocen M, Šestan A, Novak S. W2C-reinforced tungsten prepared using different precursors. Ceramics International 2019;45(6):7995–9.
[21] Deng HW, Xie ZM, Wang YK, Liu R, Zhang T, Hao T et al. Mechanical properties and thermal stability of pure W and W-0.5 wt%ZrC alloy manufactured with the same technology. Materials Science and Engineering: A 2018;715:117–25.
[22] Antusch S, Reiser J, Hoffmann J, Onea A. Refractory Materials for Energy Applications. Energy Technol. 2017;5(7):1064–70.
[23] Schade P. 100 years of doped tungsten wire. International Journal of Refractory Metals and Hard Materials 2010;28(6):648–60.
[24] Pink E, Bartha L (eds.). The metallurgy of doped/non-sag tungsten. London: Elsevier Applied Science; 1989.
[25] Moon DM, Koo RC. Mechanism and kinetics of bubble formation in doped tungsten. Metallurgical and Materials Transactions B 1971;2(8):2115–22.

[26] Suslova A, El-Atwani O, Sagapuram D, Harilal SS, Hassanein A. Recrystallization and grain growth induced by ELMs-like transient heat loads in deformed tungsten samples. Scientific reports 2014;4:6845.
[27] Lied P, Pantleon W, Bonnekoh C, Bonk S, Hoffmann A, Reiser J et al. Comparison of K-doped and pure cold-rolled tungsten sheets: Tensile properties and brittle-to-ductile transition temperatures. Journal of Nuclear Materials 2021;544:152664.
[28] Reiser J, Rieth M, Dafferner B, Hoffmann A. Tungsten foil laminate for structural divertor applications – Basics and outlook. Journal of Nuclear Materials 2012;423(1):1–8.
[29] Pantleon W. Thermal stability of the microstructure in rolled tungsten for fusion reactors. Phys. Scr. 2021;96(12):124036.
[30] Humphreys FJ, Rollett AD, Rohrer GS. Recrystallization and related annealing phenomena. Amsterdam: Elsevier; 2017.
[31] Briant CL, Hall EL. The microstructure of rolled and annealed tungsten rod. MTA 1989;20(9):1669–86.
[32] Schade P. Potassium bubble growth in doped tungsten. International Journal of Refractory Metals and Hard Materials 1998;16(1):77–87.